

Enabling Tunable Stiffness, Adhesive Grasping, and Interaction-driven Reconfiguration: A SMP-Enhanced Fin-ray Gripper

Haotian Guo ^{1,*}, Hao Wu ^{1,*}, Yanzhe Wang ^{1,*}, Yaoting Xue ², Tuck-Whye Wong ², Tiefeng Li ² and Huixu Dong ^{1,†}

Abstract

Soft grippers offer a compelling solution for handling tasks in diverse environments due to their inherent safety and adaptability. However, enhancing their versatility, particularly in load capacity and grasping range, while minimizing actuation, remains a persistent challenge. To address this, we propose a soft gripper with reconfigurable morphology, combing structure (Finray Effect gripper), and intelligent material (Shape Memory Polymers) as a union, to achieve tunable stiffness, adhesive grasping, and interaction-driven reconfiguration. First, SMPs are integrated into both the front and back beams of the FRE fingers, enabling adhesion grasping and grasping force modulation through phase transition, respectively. Additionally, by leveraging its shape-locking capabilities through intentional environmental interactions, the gripper achieves versatile reconfiguration with a single motor. Besides, inspired by humans interacting with tools and grasping in constrained spaces, we demonstrate three extra grasping modes, including precision pinching, hooking, and corner grasping. Experimental results validate its ability to handle diverse objects, from thin sheets and small nuts to items up to 50 times its own weight. This passive reconfigurable design allows for effective handling of disparate surfaces and contours, guaranteeing safe grasping in constrained spaces. This work opens new possibilities for soft robotic hands, balancing system simplicity with versatility for a wider range of real-world applications.

Keywords: shape memory polymers, soft robotic grippers, tunable stiffness, adhesive grasping, interaction-driven reconfiguration

1. Introduction

Soft grippers have garnered significant attention for their ability to safely and adaptively grasp objects in real-world applications.¹ However, many current designs are tailored for a limited range of objects or scenarios, and struggle with items that vary greatly in scale, weight, or surface texture.^{2,3} Their inherent limitations in stiffness and restricted grasping modes make it difficult to handle larger, heavier objects that exceed the gripper's workspace or designed load capacity. Additionally, achieving stable interactions and grasps in constrained environments imposes further de-

mands on complex actuation and intricate planning, complicating the control of soft manipulators.⁴ These challenges highlight the need for enhanced design strategies to improve versatility and performance across diverse grasping tasks while maintaining low system complexity.

Recent advances in stiffness-tunable materials offer a promising pathway to extend the grasping range of traditional soft grippers, especially in enhancing their load-bearing capability. These grippers can accommodate various objects by dynamically modulating rigidity without compromising compliance, which enhances versatility

* Haotian Guo, Hao Wu, and Yanzhe Wang contribute equally to this work.

1. Grasp Lab, Department of Mechanical Engineering, Zhejiang University, Hangzhou, China. huixudong@zju.edu.cn

2. Center for X-Mechanics, Department of Engineering Mechanics, Zhejiang University, Hangzhou, China

while simplifying control, and reducing the need for extra actuation systems.^{2,5} Over the past decades, numerous stiffness-tunable technologies have emerged, including electrorheological (ER)⁶ materials, particle jamming,^{7,8} low-melting-point alloys (LMPA),⁹ shape memory alloys (SMAs)¹⁰ and polymers (SMPs).¹¹ Among these, jamming-based approaches leverage frictional locking to transition granular materials from deformable to rigid, enabling simple yet versatile grasping.^{7,8} However, their insufficient grasping force and precision hinder their suitability for fine tasks. ER-based systems demonstrate rapid response times, with the ER effect manifesting in milliseconds.^{12,13} Whereas, sustaining high stiffness demands constant high voltage, resulting in significant energy consumption.¹⁴ Moreover, their limited maximum stiffness restricts their effectiveness in high-load applications.¹³ SMAs, though offering good structural rigidity and the ability to modulate stiffness, present only a narrow ($\approx 2.3\times$) stiffness variation.¹⁵ In contrast, thermally activated SMPs provide a more promising alternative, with a tunable stiffness range from a few MPa to several GPa,² enabling them to handle diverse loads. Additionally, they maintain high stiffness at ambient temperatures, reducing energy demands. Moreover, SMPs unexpectedly exhibit adhesion capabilities through phase transitions, enriching the grasping strategies available for soft robotic hands,^{16,17} making them ideal for this study.

Another challenge in enhancing soft robotic hands' versatility and grasping capabilities involves the structural design. Various structural and actuation principles have been explored.^{1,18,19} For instance, Cui et al. developed a modular soft gripper using pneumatic actuators that independently control distance, angle, and finger flexion, expanding its grasping range through dynamic initial posture adjustment.¹ Based on the antagonistic configuration of extensor and contractor McKibben muscles, Loai et al. construct a soft robotic arm, which, when activated simultaneously, increases overall stiffness without affecting finger positioning.¹⁸ Some studies focus on anthropomorphic designs to achieve human-like dexterity. For instance, Konda et al. employed 11 twisted string actuators (TSAs) to drive a 6-DOF soft gripper, successfully replicating 31 out of 33 grasps

from the Feix GRASP taxonomy.¹⁹ Despite their advancements, such systems often require bulky and complex actuators, complicating both control and maintenance. Achieving versatile grasping with minimal actuation remains a critical issue.¹⁶ In contrast, underactuated grippers, such as Fin-Ray Effect (FRE) grippers,²⁰ or underactuated linkage grippers,²¹ aim to extend the grasping range via simplified, yet effective designs. In particular, FRE grippers have been widely used in industrial settings due to their adaptability to diverse object geometries.^{22,23} However, most underactuated grippers exhibit limited grasping modes and are often tailored for specific loading ranges, limiting their ability to handle the diversity of objects encountered in daily scenarios.^{20,24} As such, there is a growing need for soft grippers capable of handling a broader range of forces and offering more diverse grasping modes to meet the demands of varied task environments.

Motivated by these unresolved issues, this study presents a novel gripper that is actuated with one motor. This design achieves versatile grasping with minimal actuation by fully leveraging the adhesion and tunable stiffness properties of SMPs. First, SMPs are strategically placed on two contact surfaces of the FRE structure. The front SMP layer permits extra adhesion-based grasping while the dorsal SMPs enable stiffness modulation to handle wider forces, reduce motor load, and improve precision. Inspired by human grasping in various scenarios, the gripper can dynamically reconfigure its morphology through intelligent interactions with the environment, further expanding its grasping modes. We highlight the key novelties of our work. **Foremost**, the core contribution lies in developing a novel soft gripper actuated by a single motor, which remarkably enables diverse grasping across a wide range of objects and constrained environments, offering significant potential for applications concurrently requiring compliance and precision. In particular, the contributions of this work are three-fold. **First**, we introduce a novel SMP-enhanced soft FRE gripper with stiffness modulation and adhesion-based grasping capabilities. This integration leverages the unique properties of SMPs to extend the gripper's adaptability and grasping versatility. **Second**, the gripper achieves flexi-

ble reconfiguration through deliberate interactions with the environment, where new morphology is maintained through SMPs' Rubber-to-Glass Transition (R2G). The shape fixation ratio is quantitatively evaluated, demonstrating the gripper's ability to reconfigure. **Third**, a human-inspired segmented stiffness modulation strategy is proposed, enabling diverse grasping modes, including precision pinching, hooking, and corner grasping. Experimental results validate the gripper's outstanding performance and versatility across varied physical environments. These innovations highlight the versatility and efficiency of the SMP-enhanced FRE gripper, providing an adaptable solution for robotic applications that require multi-functional grasping capabilities.

2. Characterization of the SMP Material

Thermal-responsive SMPs exhibit a highly tunable elastic modulus, temporary shape-locking capability, and permanent shape-memory effect when transitioning between different phases.²⁵ The stiffness ranges from surpassing 1GPa in the glassy state to around 1MPa in the rubbery state, dropping by three orders of magnitude. Additionally, deformation in the rubbery state can be retained through R2G transition, termed shape-locking. Upon reheating to temperatures surpassing the T_g , the polymer reverts to its primary configuration, demonstrating the shape-memory effect. The variance in stiffness enables SMPs to provide reliable locking and easy embedding of objects, making them ideal for applications requiring variable stiffness and surface adhesion. Prior research has predominantly focused on one single aspect of SMPs, either adhesion or variable stiffness characteristics. The work aims to fully leverage these properties by integrating them with a passive shape-adaptive gripper to enhance its versatility in grasping and manipulation.

2.1. Material and sample preparation

A thermal-triggered epoxy SMP¹⁶ is employed. The fabrication process involves mixing the epoxy monomer (E44 6101) with the curing agent (JEFFAMINE D-230, Aladdin) in a mass ratio of 81:46. The mixture is cast into pre-designed silicone molds. After curing in an oven initially at

50°C for 2 hours, followed by 100°C for 2 hours, and post-curing at 130°C for another 2 hours, the SMP substrate is obtained upon demolding.

2.2. Stiffness-tunable behaviour of the SMP

To investigate the thermomechanical behaviour of the E44 SMP, we conducted dynamic mechanical analysis (DMA) with a Q800 analyzer. The temperature was raised from 20°C to 120°C at 3°C/min. Figure 1A illustrates the DMA results. The T_g of the SMP was identified at approximately 48.6°C, based on the peak of $\tan \delta$, which represents the loss modulus to storage modulus ratio. This relatively low transition temperature enables object manipulation with minimum risk of thermal damage. The storage modulus, reflecting the elastic response, decreased significantly from 1.26 GPa at room temperature to below 10 MPa at temperatures above 80°C, indicating a transition from the glassy to the rubbery state. Besides, the wide stiffness variation range of E44 SMP enables the integration of shape adaptability with load-bearing capacity. Figure 1B shows SMP's load-bearing performance under varying conditions. At room temperature, the SMP strip (20 x 100 x 3.5 mm) exhibits high stiffness, effectively resisting bending under a load of 500 g in the cantilever beam configuration and 2 kg in the simply supported beam configuration. In contrast, the bending deflection significantly increases in the rubbery state, indicating a greatly reduced stiffness and good adaptability, where the SMP merely supports 1 g in both configurations.

2.3. Adhesion evaluation of the SMP

The E44 SMP demonstrates adhesiveness via thermally responsive phase transitions. The behavior occurs following the R2G transition upon contact with the substrate, creating a robust mechanical interlock with the surface. The SMP reverts to its initial configuration when reheated, effectively disengaging the previously secured adhesion. The R2G mechanism allows for controlled, reversible adhesion in response to thermal stimulus. To quantify this adhesion strength, we developed a cable-based adhesion measurement platform, as depicted in Figure 2A. Here, we distinguished between the influence of target surface

texture and contour on adhesion strength. SMP samples (20 x 30 x 3 mm) were prepared following stated procedures. During each test, the sample was heated above 80°C to its rubbery state, establishing conformal adhesive contact with the target surface under a preload of 1 kg. The sample was then cooled to 30°C under the preload until it transmitted to the glassy state. An upward pull was applied using water-filled weights until detachment, with the maximum force per unit area used to calculate adhesion strength.

Figure 2B shows the adhesion measurements of the SMP on substrates with different textures. Despite variations in surface roughness, the SMP exhibited robust adhesion across all materials, with forces far exceeding the applied preload. To further explore how surface curvature affects adhesion on various object shapes, SMP samples with convex, flat, and concave surfaces were tested on objects with various surface geometries. As shown in Figure 2C, SMPs with varied shapes enable stable gripping of objects with diverse geometries, where larger contact areas result in significantly higher adhesion strength. In contrast, flat SMP surfaces exhibited notably reduced adhesion on concave or convex objects. Despite the versatility of SMP material in grasping, these results highlight optimal adhesion is highly dependent on shape conformability.

3. Construction of SMP-FR Gripper

3.1. Design of SMP-FR gripper

Integrating SMPs with FRE fingers offers a novel approach to soft gripper design. Previous study explores modulating the grasping force of Festo FRE grippers by altering the stiffness of the front beam using a jamming-based mechanism.²⁶ While SMPs outperform it by providing thermo-responsive stiffness modulation and extra reversible adhesion, they require temperatures well above the glass transition temperature (T_g) to function efficiently in practical applications. This presents a risk of potential heat damage during interactions if SMPs are positioned at the front. As prior study reveals, the virtual work of FRE structure's deformation consists of the deflection of the front beam, the deformation of the front and back beams at their joints, the compression of the

crossbeams by passive torques, and the actuation force on the clamped crossbeam that moves the entire finger.²⁷ In such closed-chain structures, stiffening either the front or back beam reduces deformation, indicating higher structural stiffness and enabling higher grasping forces. Therefore, the variable stiffness SMP is strategically placed on the back contact side of the FRE structure, with the front SMP kept thin to preserve flexibility and conformability. This arrangement entitles the finger to adhere to the object while adjusting its segmented structural stiffness. Additionally, the SMR-FR gripper can reconfigure and maintain its shape through intended interactions with the objects or environment, providing a versatile grasping and manipulating solution for a wider range of objects with varied sizes, weights, and shapes.

Figure 3A presents an overview of the proposed SMP-FRE gripper, comprising two identical FRE fingers. A single stepper motor actuates the gripper through a linkage-based transmission, enabling a 180° range of motion from fully open to fully closed. Each finger contains dual SMP material layers, corresponding electroheat layers, and K-type thermocouples. The segmented electroheat pieces, each rated at 5W, enable independent heating of the SMP sections adhering to Joule's law Joule heating. Meanwhile, 8-channel K-type thermocouples, operating at 30Hz, monitor the temperature of each SMP segment to ensure precise local stiffness regulation and operational safety. Figures 3C and D detail the gripper's geometric dimensions and electronic control system. A PID controller modulates individual heating elements through PWM to maintain the desired temperatures.

3.2. Fabrication

Traditionally, fabricating SMP separately and subsequently attaching it to TPU introduces interfacial mechanical weaknesses, as the adhesive layer can serve as a plane of discontinuity, leading to stress concentrations and micro-crack propagation.²⁸ To address this, we opt for direct curing of E44 SMP onto the TPU substrate, allowing for uniform stress distribution and forming a stronger molecular bond between the SMP and TPU, which brings about improved structural integrity and durability.

The detailed fabrication process is shown in Figure 4. First, the flexible TPU skeleton and crossbeams are 3D printed using a Multi Jet Fusion (MJF) machine (HP) with TPU01 material. Thermocouples are affixed to the TPU skeleton before pouring the SMP to avoid temperature estimation errors due to thermal transmission delays. For the front beam, where surface smoothness is critical for adhesion-based grasping, the electro-heat layer is pre-placed on the skeleton surface. The SMP material is then cured on both the front and back beams following the mentioned curing conditions, with customized supports to prevent thermal deformation and ensure proper horizontal alignment. Finally, an epoxy adhesive secures the electroheat layer to the back beam of the FRE finger, and the assembly is completed by attaching the TPU crossbeams to the FRE skeleton.

4. Experiments and Results

The SMP-FR robotic system, which integrates a 6-DOF robotic arm (UR5) with the proposed gripper, was designed to evaluate its enhanced versatility in grasping and manipulation. Specifically, the experiments assess improvements in load capacity, compliance across different force ranges, and the diversity of grasping modes available. Additionally, human-inspired strategies are explored for manipulating complex objects and grasping in confined environments.

4.1. Shape fixation and recovery assessment

The SMP-FR gripper can reconfigure itself through intentional interactions with the environment. The ability to maintain a modified shape after interaction and thermally recover to its original form is essential for stable operation and reusability. This section quantitatively evaluates the finger's shape fixation and recovery abilities under various interaction conditions. As shown in Figure 5A, a single SMP-FR finger is driven to interact with a plane. In particular, we investigate how contact angle and depth affect the ratio by measuring the displacement of the beam joints compared to the initial state.

The shape fixation experiment begins by heating the finger to above T_g , with the initial positions recorded. Upon the fingertip's contact with the

plane, a downward load is applied until a predefined contact depth is reached. The joint positions in the contact state are recorded once the temperature reaches room temperature. The finger is then lifted from the surface, with the new configuration measured. By contrast, the shape recovery process starts from this locked state. The finger autonomously returns to its original configuration when reheated. Joint positions are continuously tracked throughout the recovery phase. Here, we define two metrics, the shape fixation ratio (SFR) and the shape recovery ratio (SRR), to quantify shape retention and recovery capabilities, namely:

$$\begin{aligned} \text{SFR} &= \frac{1}{N} \sum_{i=1}^N \frac{\|\mathbf{p}_i^{\text{loc}} - \mathbf{p}_i^{\text{ini}}\|}{\|\mathbf{p}_i^{\text{con}} - \mathbf{p}_i^{\text{ini}}\|} \\ \text{SRR} &= \frac{1}{N} \sum_{i=1}^N \frac{\|\mathbf{p}_i^{\text{rec}} - \mathbf{p}_i^{\text{loc}}\|}{\|\mathbf{p}_i^{\text{loc}} - \mathbf{p}_i^{\text{ini}}\|} \end{aligned} \quad (1)$$

where $\|\cdot\|$ represents the Euclidean distance, N is the number of joints, $\mathbf{p}_i^{\text{ini}}$, $\mathbf{p}_i^{\text{con}}$, $\mathbf{p}_i^{\text{loc}}$, and $\mathbf{p}_i^{\text{rec}}$ denote the initial joint position, joint position during contact, locked joint position, and joint position during recovery, respectively.

Results of the shape fixation experiment are presented, as seen in Figure 5B. Three contact angles (0° , 30° , and 60°) and four loading depths (3mm, 6mm, 9mm, and 12mm) are considered. The results demonstrate that with only stiffness modulation of the dorsal SMP, the configuration of the FRE finger during various interaction scenarios can be well maintained. Throughout the tests, the structural shape fixation ratio remained above 70%, even during large deformations. The ratio exceeds approximately 85% when the contact depth is less than 6 mm. As contact angles and loading depths increase, the shape fixation ratio decreases accordingly. This is due to the significant compression of the crossbeams by passive torques during large deformations, which cannot be ignored or locked, leading to a discrepancy between the locked and interaction states. These results validate the proposed hand's ability to achieve reconfigurable interactions with the environment, enhancing its reliability in confined environments for successful grasping.

Shape recovery experiment following deformation at 30° and a loading depth of 12mm is further demonstrated, where a shape recovery ra-

tio of 95% is set as the acceptable operational threshold. The desired temperature is set to 80°C, and Figure 5C shows the heating curve of one SMP during the heating. The SMP reaches the T_g at 79.45 seconds, and the whole finger recovers its shape in 318.95 seconds, with the recovered configuration closely matching the initial state. This result demonstrates SMP-FR's excellent structure memory and recovery capabilities under controlled heating conditions, ensuring high operational efficiency and reliability over multiple usage cycles.

4.2. Enhanced shape adaptability and load handling capabilities

The FRE gripper, known for its inherent compliance, typically exhibits limitations regarding its load capacity and stability. The incorporation of SMP material can significantly expand its structural stiffness range, which allows the gripper to augment its load capacity and stability without sacrificing adaptivity, essential for manipulating objects with varying weights and shapes.

The shape adaptability and load capacity of the SMP-FR gripper were evaluated through grasping tests in both low and high-stiffness modes. Figure 6A shows the gripper conforming to various objects, highlighting its gentle handling capabilities and good shape adaptability. Figure 6B shows its ability to handle items that require sufficient tip stiffness. In Figure 3C, the gripper successfully lifted 1000 g and 500 g weights in high stiffness. While it can merely lift 100 g weight, with the 200 g weight slipping in low stiffness. Figure 6D illustrates the gripper's crushing force in high stiffness, greatly deforming a soda can, in contrast to the low stiffness setting, which left the can undamaged. The experiment highlights the great stiffness variance of the SMP-FR finger and its capability of handling diverse objects beyond what ordinary fin rays can achieve.

4.3. Interaction-driven reconfiguration for enhanced versatility

Conventional FRE grippers rely on passive deformation to envelop various objects but struggle with flat, thin, or tiny objects on planar surfaces and large convex objects due to the lack of special-

ized grasping mechanisms. Additionally, engaging with larger convex objects can be challenging due to an insufficient grasping angle. The integration of SMP significantly enhances performance. For large-radius, thin, or tiny objects, the back beam remains stiff to apply sufficient preload, while the front beam's adhesion secures the grip. For concave surfaces, heating the gripper above T_g allows the front beam to conform to the shape, and once cooled, the front SMP provides stable adhesion. This flexibility enables conformal adhesive contact with diverse surface shapes, improving grasp stability and robustness. As shown in Figure 7A, the gripper successfully grasped an acrylic semi-sphere, a basketball, a 14-inch plate, an A4 sheet of paper, a thin ID card, and M5 nuts.

The dorsal SMPs significantly enhance the grasping and manipulation capabilities of the gripper by enabling interaction-driven reconfiguration. We simplify this interaction by considering a two-phalange gripper, one soft and one rigid, as illustrated in Figure 7B. Soft robots, due to their joint compliance, effectively interact with their environment and achieve grasping under environmental constraints. However, their grasping force is entirely determined by joint stiffness, often leading to failure due to insufficient tip stiffness. Conversely, conventional rigid grippers struggle with environmental interaction and require precise kinematic planning for successful grasping, risking damage to the hand. We experimentally validated the benefits of variable stiffness for the FRE hand. As shown in Figure 7C, we measured improvements in shear grasping force when attempting to grasp a steel ball weighing 1180 g. Both the stiff and flexible states experienced failure due to insufficient contact area and grasping force. In contrast, our proposed gripper employs a soft interaction-stiff grasping strategy, significantly increasing contact area while maintaining stability and load capacity during grasping. Additionally, variable stiffness aids in operating tools in real-world scenarios. Inspired by human grasping and using configurations, we demonstrate the gripper's capabilities with a hand drill. To stabilize the grasp without triggering the switch, we selectively heated the middle section of the back beam before grasping to reduce interaction force. After cooling, we enhanced grasp stability. As we

approached the target, we further closed the gripper to activate the switch while ensuring stability. Using our proposed human-like grasping and operation strategy, we successfully drilled into a 3 mm thick wooden board.

Furthermore, we evaluated the grasping performance of the proposed gripper using human-inspired interaction strategies in various constrained scenarios. As previously noted, grasping thin objects from flat surfaces often requires specialized designs and careful grasp planning.⁴ The proposed hand utilizes reconfigurable and lockable soft interactions with the environment, allowing for flexible change in its workspace and achieving precise pinching actions through scooping. Figure 7D illustrates the gripper successfully picking a thin plate, a pen, and a slot nut from a table. Moreover, when both fingers are in a flexible state, the interaction with the environment can dynamically alter the tip orientation, allowing for a human-like hook configuration that stably manages objects with handles. This configuration has been further validated for shoulder dumbbells weighing 2.5 kg (50 times its weight). Besides, inspired by human grasping objects trapped in corners, the tip of the FRE finger can engage with walls, allowing it to slide into gaps between objects and the wall. During this adaptive closing process, the hand effectively translates the object and achieves a stable grasp upon cooling into a rigid state. This approach highlights the hand's versatility in real-world scenarios, ensuring secure handling in complex environments.

5. Conclusion

To conclude, this study introduces a novel paradigm that utilizes the thermo-responsive stiffness and reversible adhesion of SMP materials to augment the grasping modality in FRE gripper design. The integration of SMPs not only expands the range of stiffness variations by tens of times while preserving its adaptability but also facilitates the capability of grasping large-radius, thin, or tiny objects through adhesion-based mechanisms. Besides, the gripper excels at handling a broad spectrum of objects while also securing excellent grasping performance in constrained environments. Inspired by human grasping and manipulation strategies, the gripper actively mod-

ifies its configuration to handle complex tasks with minimal complexity. This work proposes a novel solution for multifunctional grasping in soft robotics, addressing the pressing need for compliance, precision, and load-carrying in real-world applications. Future efforts will explore the integration of active cooling mechanisms to improve cooling efficiency, as well as the development of autonomous reconfiguration strategies based on theoretical modeling, pushing the boundaries of reconfigurable robotic systems.

6. Acknowledgements

The authors gratefully acknowledge the financial support from the National Key Research and Development Program of China (Grant no. 2023YFB4704700) and the pioneer" R&D Program of Zhejiang (Grant no. 2023C03007).

7. Author Disclosure Statement

No competing financial interests exist.

8. Supplementary Material

Supplementary Movie S1
Supplementary Movie S2
Supplementary Movie S3
Supplementary Movie S4
Supplementary Movie S5

References

- ¹ Y. Cui, X.-J. Liu, X. Dong, J. Zhou, and H. Zhao, "Enhancing the Universality of a Pneumatic Gripper via Continuously Adjustable Initial Grasp Postures," *IEEE Transactions on Robotics*, vol. 37, pp. 1604–1618, Oct. 2021.
- ² Y. Zhang, N. Zhang, H. Hingorani, N. Ding, D. Wang, C. Yuan, B. Zhang, G. Gu, and Q. Ge, "Fast-Response, Stiffness-Tunable Soft Actuator by Hybrid Multimaterial 3D Printing," *Advanced Functional Materials*, vol. 29, p. 1806698, Apr. 2019.
- ³ Y. Yang, Y. Chen, Y. Li, M. Z. Chen, and Y. Wei, "Bioinspired Robotic Fingers Based on Pneumatic Actuator and 3D Printing of Smart Ma-

- terial,” *Soft Robotics*, vol. 4, pp. 147–162, June 2017.
- ⁴ V. Babin and C. Gosselin, “Picking, grasping, or scooping small objects lying on flat surfaces: A design approach,” *The International Journal of Robotics Research*, vol. 37, no. 12, pp. 1484–1499, 2018.
 - ⁵ M. Manti, V. Cacucciolo, and M. Cianchetti, “Stiffening in soft robotics: A review of the state of the art,” *IEEE Robotics Automation Magazine*, vol. 23, no. 3, pp. 93–106, 2016.
 - ⁶ T. C. Halsey, “Electrorheological fluids,” *Science*, vol. 258, no. 5083, pp. 761–766, 1992.
 - ⁷ G. B. Crowley, X. Zeng, and H.-J. Su, “A 3D Printed Soft Robotic Gripper With a Variable Stiffness Enabled by a Novel Positive Pressure Layer Jamming Technology,” *IEEE Robotics and Automation Letters*, vol. 7, pp. 5477–5482, Apr. 2022.
 - ⁸ E. Brown, N. Rodenberg, J. Amend, A. Mozeika, E. Steltz, M. R. Zakin, H. Lipson, and H. M. Jaeger, “Universal robotic gripper based on the jamming of granular material,” *Proceedings of the National Academy of Sciences*, vol. 107, no. 44, pp. 18809–18814, 2010.
 - ⁹ R. Zhao, Y. Yao, and Y. Luo, “Development of a Variable Stiffness Over Tube Based on Low-Melting-Point-Alloy for Endoscopic Surgery,” *Journal of Medical Devices*, vol. 10, p. 021002, 05 2016.
 - ¹⁰ W. Wang, C. Y. Yu, P. A. Abrego Serrano, and S.-H. Ahn, “Shape Memory Alloy-Based Soft Finger with Changeable Bending Length Using Targeted Variable Stiffness,” *Soft Robotics*, vol. 7, pp. 283–291, June 2020.
 - ¹¹ A. Firouzeh, M. Salerno, and J. Paik, “Stiffness control with shape memory polymer in under-actuated robotic origamis,” *IEEE Transactions on Robotics*, vol. 33, no. 4, pp. 765–777, 2017.
 - ¹² A. Tonazzini, A. Sadeghi, and B. Mazzolai, “Electrorheological valves for flexible fluidic actuators,” *Soft Robotics*, vol. 3, no. 1, pp. 34–41, 2016.
 - ¹³ H. Jing, L. Hua, F. Long, B. Lv, B. Wang, H. Zhang, X. Fan, H. Zheng, C. Chu, G. Xu, J. Guo, A. Sun, and Y. Cheng, “Variable stiffness and fast-response soft structures based on electrorheological fluids,” *J. Mater. Chem. C*, vol. 11, no. 35, 2023.
 - ¹⁴ T. Atakuru, G. Züngör, and E. Samur, “Layer Jamming of Magnetorheological Elastomers for Variable Stiffness in Soft Robots,” *Exp Mech*, vol. 64, pp. 393–404, Apr. 2024.
 - ¹⁵ J. Shintake, B. Schubert, S. Rosset, H. Shea, and D. Floreano, “Variable stiffness actuator for soft robotics using dielectric elastomer and low-melting-point alloy,” in *2015 IEEE/RSJ International Conference on Intelligent Robots and Systems (IROS)*, pp. 1097–1102, 2015.
 - ¹⁶ C. Linghu, S. Zhang, C. Wang, K. Yu, C. Li, Y. Zeng, H. Zhu, X. Jin, Z. You, and J. Song, “Universal SMP gripper with massive and selective capabilities for multiscaled, arbitrarily shaped objects,” *Science Advances*, vol. 6, no. 7, p. eaay5120, 2020.
 - ¹⁷ J. K. Park, J. D. Eisenhaure, and S. Kim, “Reversible Underwater Dry Adhesion of a Shape Memory Polymer,” *Advanced Materials Interfaces*, vol. 6, no. 1801542, 2019.
 - ¹⁸ L. A. Al Abeach, S. Nefti-Meziani, and S. Davis, “Design of a Variable Stiffness Soft Dexterous Gripper,” *Soft Robotics*, vol. 4, pp. 274–284, Sept. 2017.
 - ¹⁹ R. Konda, D. Bombara, S. Swanbeck, and J. Zhang, “Anthropomorphic Twisted String-Actuated Soft Robotic Gripper With Tendon-Based Stiffening,” *IEEE Transactions on Robotics*, vol. 39, pp. 1178–1195, Apr. 2023.
 - ²⁰ J. Yao, Y. Fang, X. Yang, P. Wang, and L. Li, “Design optimization of soft robotic fingers biologically inspired by the fin ray effect with intrinsic force sensing,” *Mechanism and Machine Theory*, vol. 191, p. 105472, 2024.
 - ²¹ H. Wang, B. Gao, A. Hu, and J. He, “A variable stiffness gripper with reconfigurable finger joint for versatile manipulations,” *Soft Robotics*, vol. 10, no. 5, pp. 1041–1054, 2023. PMID: 37103972.

- ²² R. Chen, R. Song, Z. Zhang, L. Bai, F. Liu, P. Jiang, D. Sindersonberger, G. J. Monkman, and J. Guo, “Bio-Inspired Shape-Adaptive Soft Robotic Grippers Augmented with Electro-adhesion Functionality,” *Soft Robotics*, vol. 6, pp. 701–712, Dec. 2019.
- ²³ X. Liu, X. Han, W. Hong, F. Wan, and C. Song, “Proprioceptive learning with soft polyhedral networks,” *The International Journal of Robotics Research*, vol. 0, no. 0, p. 02783649241238765, 0.
- ²⁴ X. Wang, B. Wang, J. Pinskiere, Y. Xie, J. Brett, R. Scalzo, and D. Howard, “Fin-bayes: A multi-objective bayesian optimization framework for soft robotic fingers,” *Soft Robotics*, vol. 0, no. 0, p. null, 0. PMID: 38498017.
- ²⁵ Y. Xia, Y. He, F.-h. Zhang, Y. Liu, and J. Leng, “A review of shape memory polymers and composites: Mechanisms, materials, and applications,” *Advanced materials (Deerfield Beach, Fla.)*, vol. 33, p. e2000713, 09 2020.
- ²⁶ S. Kashef Tabrizian, S. Terryn, D. Brauchle, J. Seyler, J. Brancart, G. Van Assche, and B. Vanderborght, “Variable stiffness, sensing, and healing in festo’s finray gripper: An industry-driven design,” *IEEE Robotics Automation Magazine*, pp. 2–13, 2024.
- ²⁷ X. Shan and L. Birglen, “Modeling and analysis of soft robotic fingers using the fin ray effect,” *The International Journal of Robotics Research*, vol. 39, no. 14, pp. 1686–1705, 2020.
- ²⁸ H.-L. Liu, C.-L. Lin, M.-T. Sun, and Y.-H. Chang, “3D Micro-Crack Propagation Simulation at Enamel/Adhesive Interface Using FE Submodeling and Element Death Techniques,” *Ann Biomed Eng*, vol. 38, pp. 2004–2012, June 2010.
- [Figure 1 about here.]
- [Figure 2 about here.]
- [Figure 3 about here.]
- [Figure 4 about here.]
- [Figure 5 about here.]
- [Figure 6 about here.]
- [Figure 7 about here.]

List of Figures

- 1 Stiffness-tunable behaviour of the SMP material. **(A)** The DMA characterization of the E44 epoxy SMP (Test frequency 1Hz, temperature rise rate 3°C/min). **(B)** Demonstration of the stiffness variation of the thermally activated SMP material at 25 and 80°C. 12

- 2 Adhesion performance of the SMP material to objects with various materials and arbitrary shapes. **(A)** Setup for measuring the normal adhesion strength of the SMP sample. **(B)** Grip force to planar objects of different materials: wood, aluminum, ceramics, acrylic, rough glass and smooth glass (length 100mm, width 100mm, thickness 3mm). **(C)** Grip force of SMP with flat, concave and convex surfaces to objects with different shapes: annulus (diameter, 20mm), sphere (diameter, 100mm), concave (diameter, 182.5mm), convex (diameter, 182.5mm), sawtooth (triangular serrations with a side length of 1 mm), wave (semicircular waves with a diameter of 1 mm). 13

- 3 Schematic diagram of the SMP-FR gripper. **(A)** Illustration of the gripper's structure and workspace. **(B)** Exploded view of the SMP-FR finger. **(C)** Detailed schematic of geometric parameters. **(D)** Layout of the electronic system configuration. 14

- 4 Fabrication procedure of the SMP-FR finger. **(A)** Print the TPU skeleton with SLS and paste the thermocouples. **(B)** Mix the epoxy monomer and curing agent D-230, pour the mixture into the back beam and pre-cure in the oven at 50°C for 2 hours, cure at 100°C for 2 hours and post-cure at 130°C for 2 hours. **(C)** Integrate SMP with the front beam in the same way, meanwhile insert the electroheat film inside the material. **(D)** Assemble the fin ray finger with segmented electroheat film and TPU crossbeams. 15

- 5 Shape fixation and recovery capability experiments. **(A)** Schematic of the experimental principle, including quantitative loading conditions, interaction process, and description of evaluation metrics. **(B)** Results of the shape locking capability experiment, demonstrating SFR measurements of the SMP-FR finger at various interaction angles and depths. **(C)** Results of the shape recovery capability experiment, demonstrate SRR measurements of the SMP-FR finger as it autonomously returns to its initial state after heating from the locked state, along with the corresponding temperatures. 16

- 6 Demonstration of good shape adaptability and high load capacity of the SMP-FR gripper. **(A)** Low stiffness mode: The SMP-FR gripper conforms to objects with various shapes including a tape measure (83.5g), a mooncake (82.8g), a pear (280.7g) and a tennis (58.6g), showcasing its adaptability for gentle handling. **(B)** High stiffness mode: The SMP-FR gripper exhibits sufficient load-bearing capacity and gripping force to securely grasp objects including a screwdriver (25.5g), a flange (304.3g), a mental block (423.8g) and a mental can (548.8g). **(C)** Load-bearing capacity comparison: at high stiffness, the gripper can successfully lift 500g and 1000g weights, whereas, at low stiffness, it can only securely grasp 100g weights, with 200g weights slipping. **(D)** Impact assessment on a soda can: when applying maximum force, high stiffness results in significant deformation, while low stiffness preserves the can's integrity. 17

- 7 Demonstration of the enhanced capabilities and strategies for object grasping and manipulation. **(A)** Grasping of an acrylic semi-sphere with a diameter of 300 mm (296g), a basketball with a diameter of 246mm (600g), a 14-inch plate (540g), A sheet of A4 paper (4.5g), an ID card (6.4g) and M5 nuts (one weighting 6.6g) with SMP adhesion. **(B)** Comparison of interaction mechanisms between a simplified soft and rigid gripper during object grasping from constrained surfaces. **(C)** Enhanced grasping and manipulation through sophisticated robot-object interactions. Leveraging the tunable stiffness characteristic and proper strategy, the gripper can interact with objects to achieve the grasping of a steel ball (1180g) and the manipulation of a hand drill. **(D)** Robotic Environmental Interaction for Versatile Grasping Reconfiguration. Through interacting with the desktop or box frame, the gripper can alter its configuration to perform human-like actions including precise pinching, hooking and corner grasping. 18

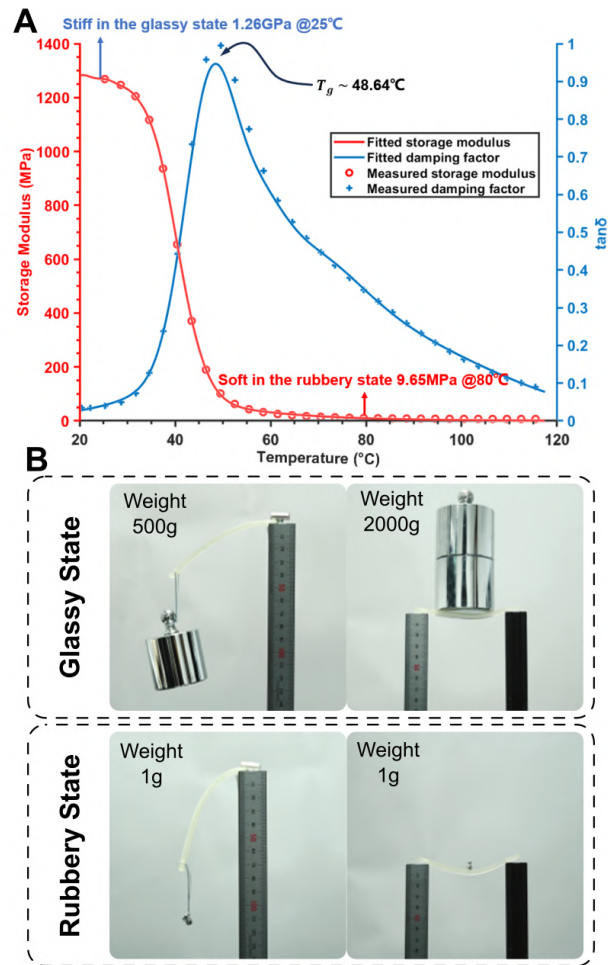


Figure 1. Stiffness-tunable behaviour of the SMP material. (A) The DMA characterization of the E44 epoxy SMP (Test frequency 1Hz, temperature rise rate 3°C/min). (B) Demonstration of the stiffness variation of the thermally activated SMP material at 25 and 80°C.

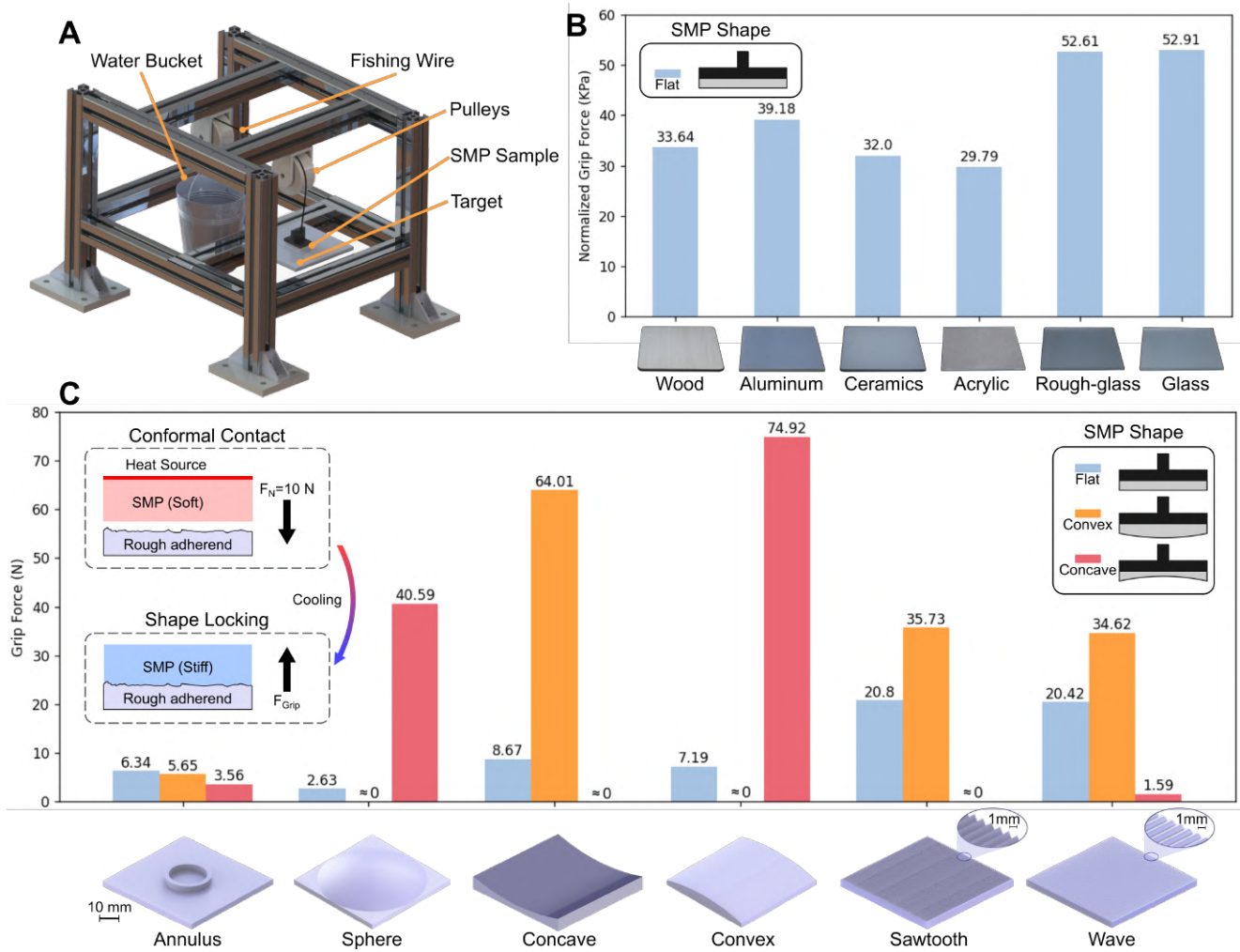


Figure 2. Adhesion performance of the SMP material to objects with various materials and arbitrary shapes. **(A)** Setup for measuring the normal adhesion strength of the SMP sample. **(B)** Grip force to planar objects of different materials: wood, aluminum, ceramics, acrylic, rough glass and smooth glass (length 100mm, width 100mm, thickness 3mm). **(C)** Grip force of SMP with flat, concave and convex surfaces to objects with different shapes: annulus (diameter, 20mm), sphere (diameter, 100mm), concave (diameter, 182.5mm), convex (diameter, 182.5mm), sawtooth (triangular serrations with a side length of 1 mm), wave (semicircular waves with a diameter of 1 mm).

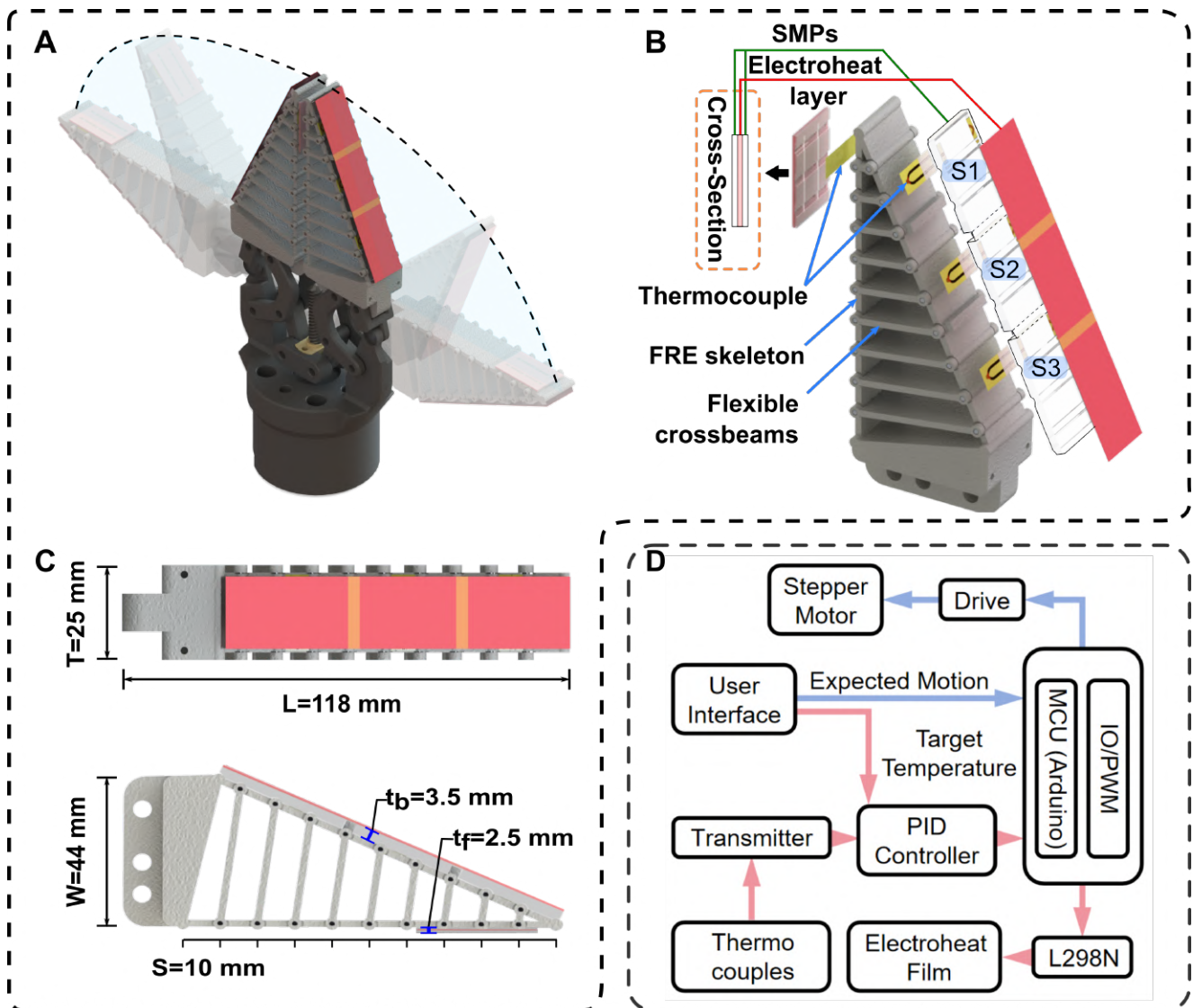


Figure 3. Schematic diagram of the SMP-FR gripper. (A) Illustration of the gripper's structure and workspace. (B) Exploded view of the SMP-FR finger. (C) Detailed schematic of geometric parameters. (D) Layout of the electronic system configuration.

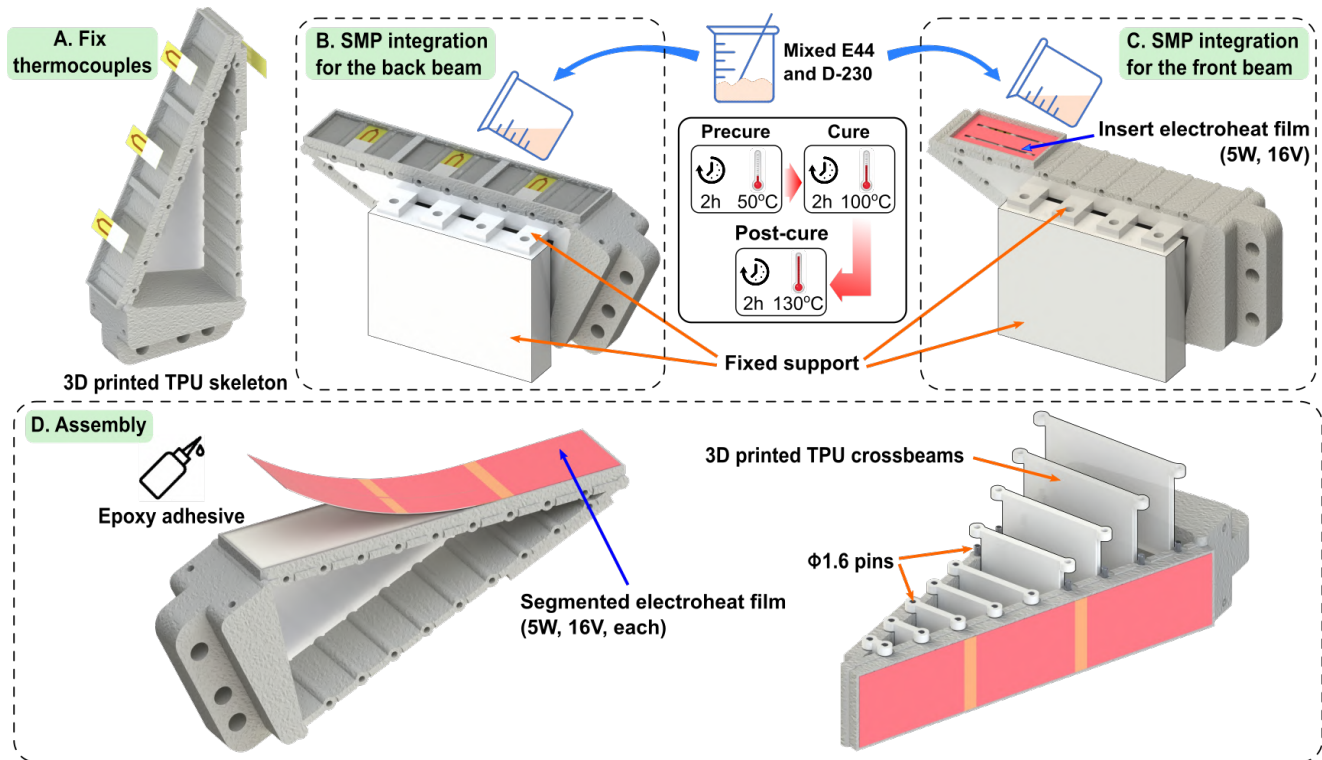


Figure 4. Fabrication procedure of the SMP-FR finger. (A) Print the TPU skeleton with SLS and paste the thermocouples. (B) Mix the epoxy monomer and curing agent D-230, pour the mixture into the back beam and pre-cure in the oven at 50°C for 2 hours, cure at 100°C for 2 hours and post-cure at 130°C for 2 hours. (C) Integrate SMP with the front beam in the same way, meanwhile insert the electroheat film inside the material. (D) Assemble the fin ray finger with segmented electroheat film and TPU crossbeams.

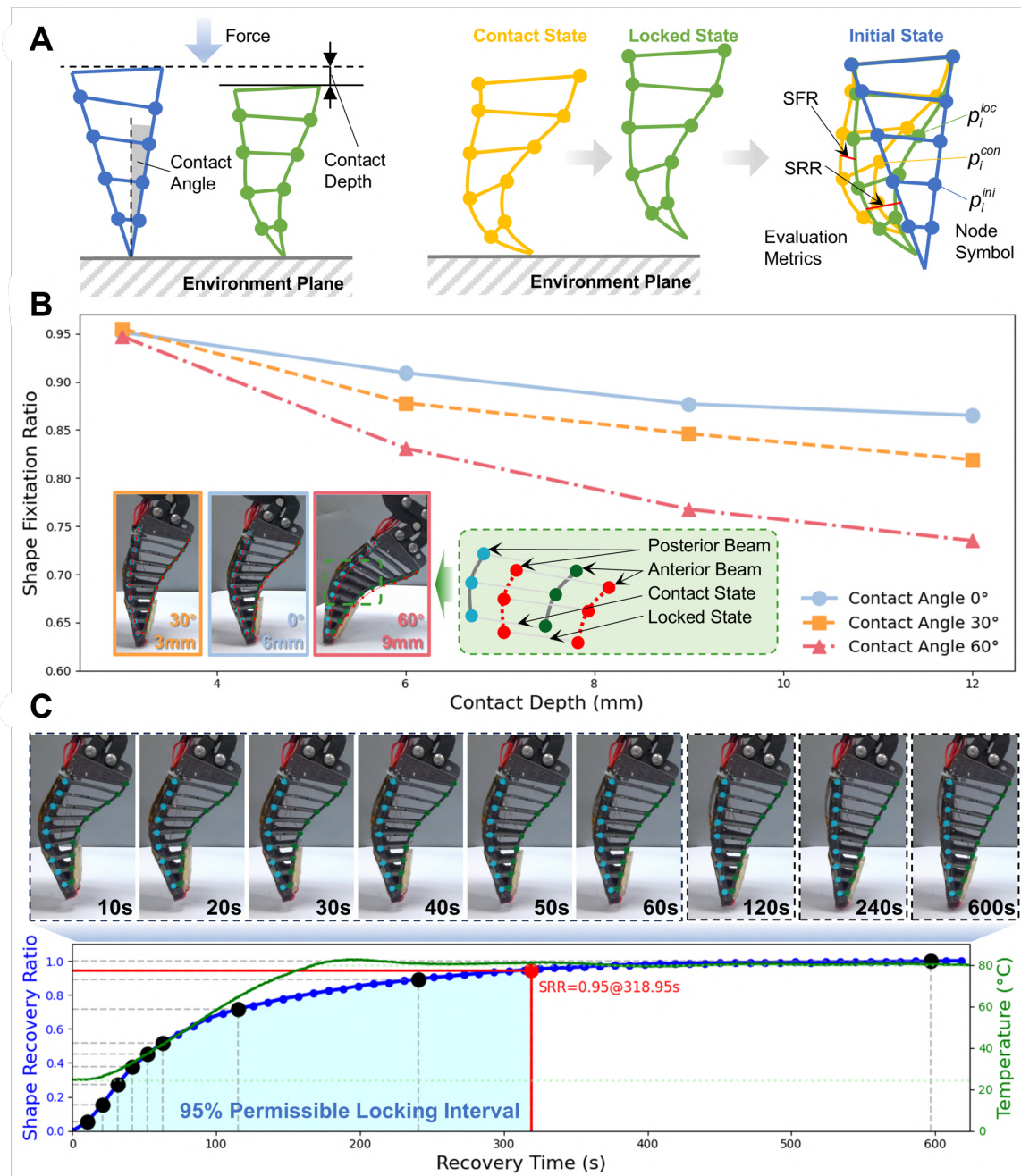


Figure 5. Shape fixation and recovery capability experiments. (A) Schematic of the experimental principle, including quantitative loading conditions, interaction process, and description of evaluation metrics. (B) Results of the shape locking capability experiment, demonstrating SFR measurements of the SMP-FR finger at various interaction angles and depths. (C) Results of the shape recovery capability experiment, demonstrate SRR measurements of the SMP-FR finger as it autonomously returns to its initial state after heating from the locked state, along with the corresponding temperatures.

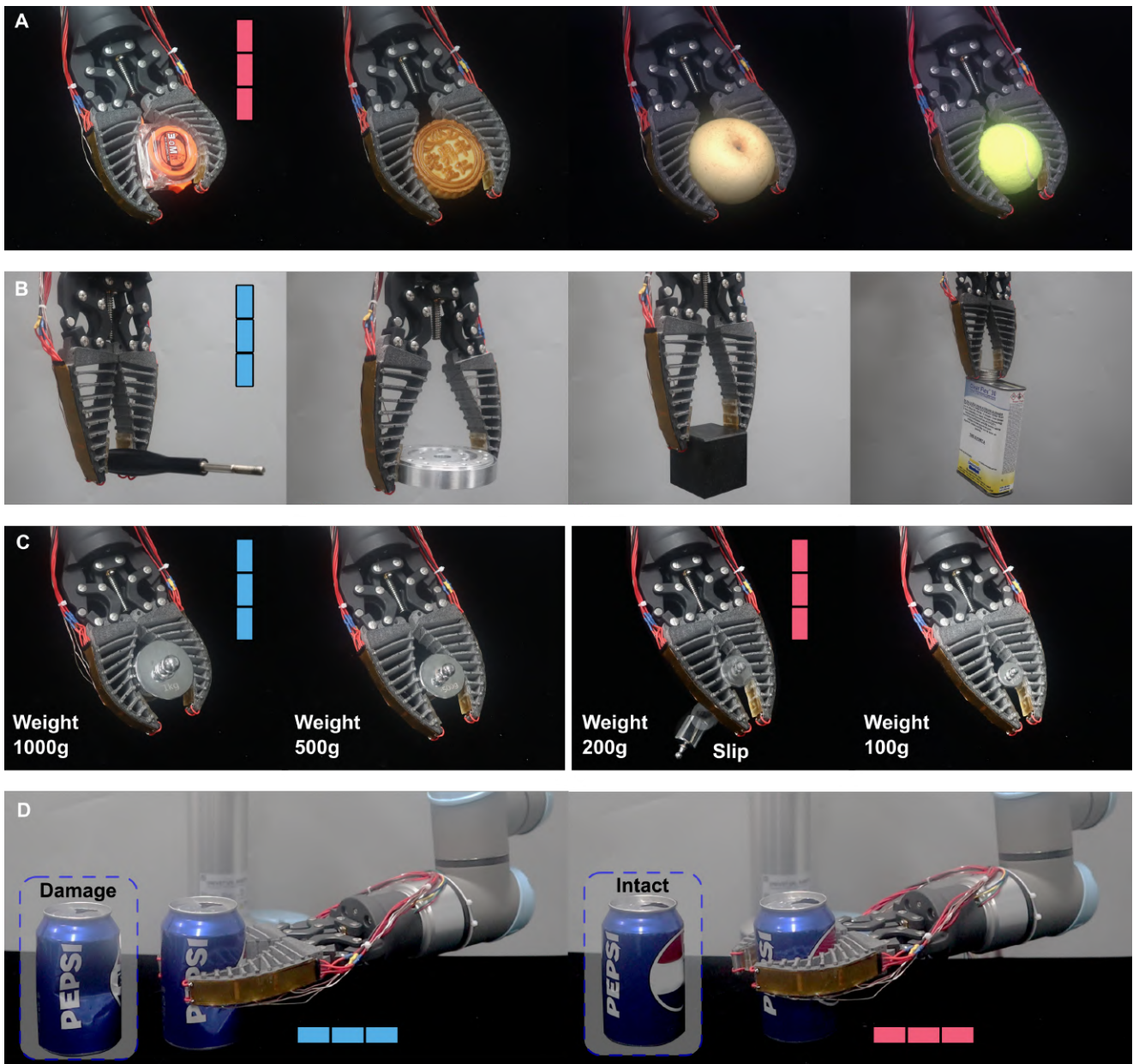


Figure 6. Demonstration of good shape adaptability and high load capacity of the SMP-FR gripper. **(A)** Low stiffness mode: The SMP-FR gripper conforms to objects with various shapes including a tape measure (83.5g), a mooncake (82.8g), a pear (280.7g) and a tennis (58.6g), showcasing its adaptability for gentle handling. **(B)** High stiffness mode: The SMP-FR gripper exhibits sufficient load-bearing capacity and gripping force to securely grasp objects including a screwdriver (25.5g), a flange (304.3g), a metal block (423.8g) and a metal can (548.8g). **(C)** Load-bearing capacity comparison: at high stiffness, the gripper can successfully lift 500g and 1000g weights, whereas, at low stiffness, it can only securely grasp 100g weights, with 200g weights slipping. **(D)** Impact assessment on a soda can: when applying maximum force, high stiffness results in significant deformation, while low stiffness preserves the can's integrity.

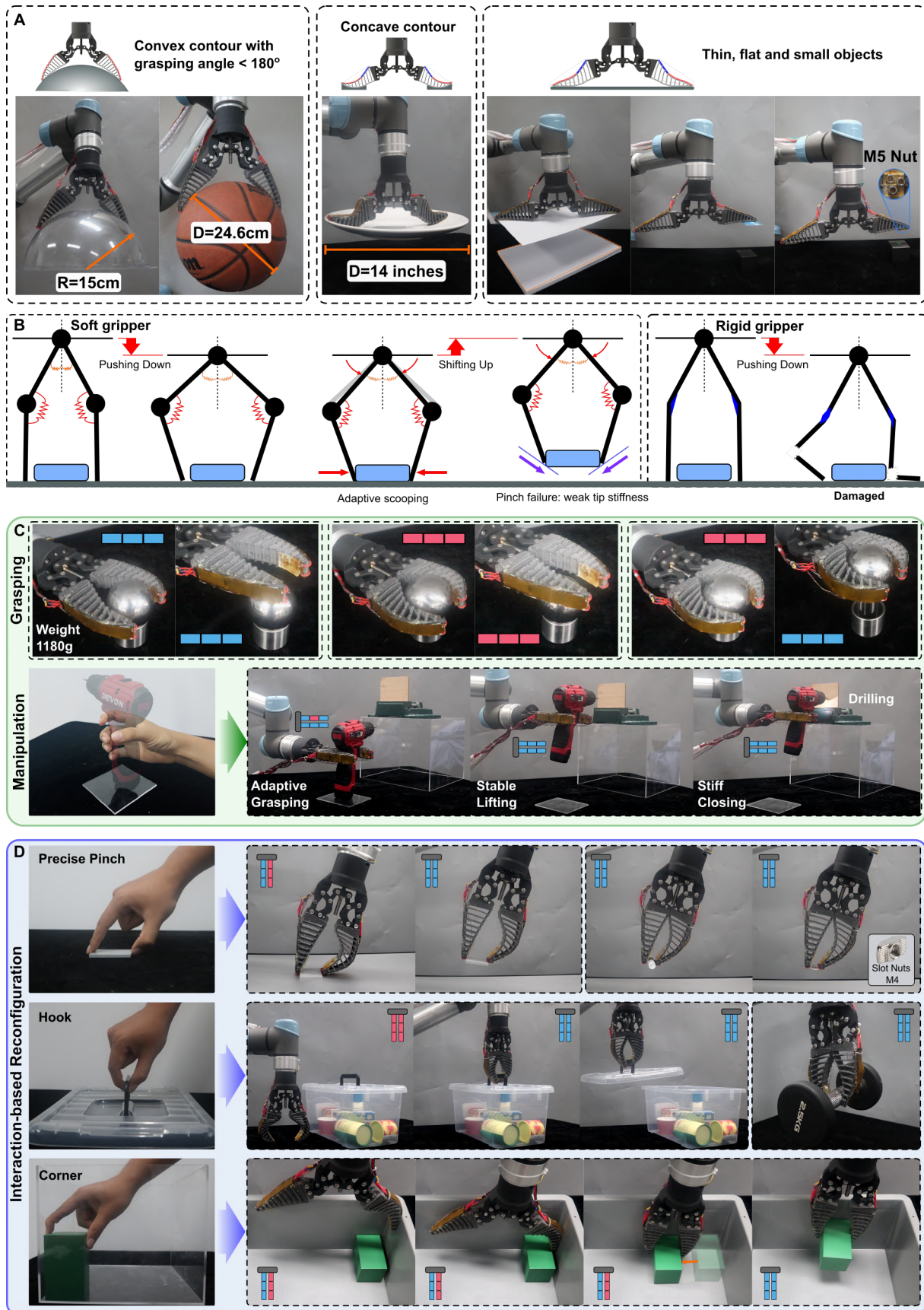


Figure 7. Demonstration of the enhanced capabilities and strategies for object grasping and manipulation. **(A)** Grasping of an acrylic semi-sphere with a diameter of 300 mm (296g), a basketball with a diameter of 246mm (600g), a 14-inch plate (540g), A sheet of A4 paper (4.5g), an ID card (6.4g) and M5 nuts (one weighting 6.6g) with SMP adhesion. **(B)** Comparison of interaction mechanisms between a simplified soft and rigid gripper during object grasping from constrained surfaces. **(C)** Enhanced grasping and manipulation through sophisticated robot-object interactions. Leveraging the tunable stiffness characteristic and proper strategy, the gripper can interact with objects to achieve the grasping of a steel ball (1180g) and the manipulation of a hand drill. **(D)** Robotic Environmental Interaction for Versatile Grasping Reconfiguration. Through interacting with the desktop or box frame, the gripper can alter its configuration to perform human-like actions including precise pinching, hooking and corner grasping.